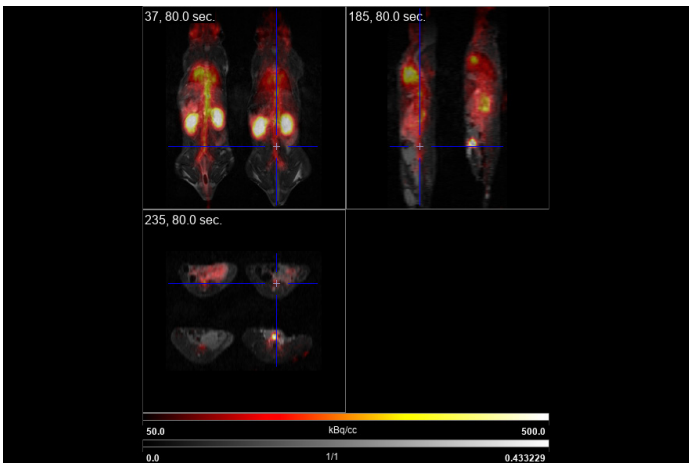

Multi-Animal Simultaneous PET/MR Imaging

Iris Y Zhou[1], Christian T Farrar[1], Joseph Mandeville[1], Michael S. Placzek[1], Nicholas J Rotile[1], Cesar Molinos Solsona[2], Todd Sasser[2], Shadi A Esfahani[1], Michael Heidenreich[2] and Peter Caravan[1]

[(1)] The Athinoula A. Martinos Center for Biomedical Imaging, The Institute for Innovation in Imaging, Massachusetts General Hospital and Harvard Medical School, 149 Thirteenth Street, Charlestown, Massachusetts 02129, USA
[(2)] Bruker BioSpin, Preclinical Imaging, Billerica, MA, USA

Introduction

Common applications for preclinical PET include tracer development and use of specialized animal strains (knock-out mice or disease models) to investigate novel drugs or address biological questions that are not easily studied in humans. Frequently, developmental tracers are initially evaluated in small test batches before scaling up production. Production of multiple small batch tracers often using iterative chemistries in developmental phases can be costly. When using short half-life isotopes (e.g. 11C half-life = 20-minutes) a single batch of tracer may only be enough for a single scan before tracer activity decays. Even when using the most commonly synthesized 11C radioisotopes, radiochemistry and cyclotron costs present a cost burden. Studies of disease progression and evaluation of therapeutic interventions often employ longitudinal designs with control groups and 6-12 animals per cohort. Where kinetic details are desired, scan times required may reach 60 minutes or longer, so it not feasible to perform multiple scans using one synthesis of radiotracer. Typically, the total dose available is not a limiting factor in small-animal studies, and a single synthesis of radiotracer provides enough dose for many animals. For these reasons, researchers in preclinical PET frequently attempt to maximize efficiency by performing multi-animal PET scans.

Multi-mouse imaging has of course also a great advantage with longer lived isotopes as it increases throughput.
Some commercial vendors have begun offering solutions for multi-animal imaging. Bruker for example supplies multi-animal cradles for both PET/MR and PET/CT, see Addendum. Still, many researchers have unique requirements for specific applications and the advent of 3D printing and prototyping has led some to begin developing custom solutions for multi animal-imaging. Until now, many reports related to multi-animal cradle prototyping have been related to studies using PET/CT. Multi-animal PET/MR imaging will have its own unique requirements.

Here we report on the development of multi-animal cradles to accommodate 2, 3, 4 and up to 6 animals during PET/MR imaging using with the Bruker BioSpec 4.7T and Bruker PET Insert 198. Custom cradles were developed to accommodate both whole body multi-animal mouse dynamic PET/MRI studies and head-to-head multi-animal mouse and rat PET/MRI brain studies. Our data shows excellent combined image quality in PET and MR for multi-animal imaging and with demonstrated application in multi-animal dynamic imaging. To our knowledge this is the first report for routine high-throughput PET in this platform.

PET/MRI Instrumentation

The Bruker BioSpec 47/40USR and Bruker PET Insert located in the Martinos Center for Biomedical Imaging were used for multi-animal/multi-modal scans, see Figure 1. The Center serves a body of researchers with regular use for both PET/MR and MR only protocols. The PET Insert system fits within the MR BGA20 gradient and has an inner diameter of 114 mm and an 80 × 150 mm FOV. See ref. 1 for a NEMA characterization of the PET Insert. For whole body dynamic PET studies, the Bruker 82 mm volume coil (RF RES 200 1H 112/86 QSN) is typically used.

Figure 1

Figure 1. Top: PET Insert sitting on support cart with all PET electronics. Bottom PET Insert being used inside the magnet bore of the Biospec 4.7 T.

Multi-Animal PET/MRI Studies

Three multi-animal experiments are presented in this section to illustrate different high throughput scenarios of preclinical simultaneous PET/MRI. The first one covers the case of total body - mouse dynamic imaging to investigate the kinetics of a F18 amino acid-based tracer. The second one demonstrates a 6-mouse neurological study using a C11 raclopride. The third and final example deals with a neurological study involving 2 rats. The first study is used to cover in detail the workflow whereas the second and third are presented in a more concise way.

Whole Body 4-Mouse Dynamic Imaging

Method and material

Figure 2 shows a 4-mouse cradle developed at the Martinos Center for Biomedical Imaging for multi-modal PET/MR imaging using the system. The bed assemblies (2-mouse base platform with nose cone and bite bar holder, single mouse platforms with mouse nose cone and bite bar holder) components were 3D printed using standard technologies. Top mouse platforms can be added or removed to the base assembly using positioning grooves at the top of the base mouse nose cone or by dropping the top assembly into 4 tightly fitting corners provided by support bars on the lower assembly. Bite bars were constructed by attaching 3D-printed mouth bars made of polycarbonate-ISO material to gas delivery tubes used halogen-free Garolite G-10 tubing (McMaster-Carr), which provides good strength with minimal wall thickness. The 4-mouse cradle delivered gas though a single branched delivery line.

Figure 2

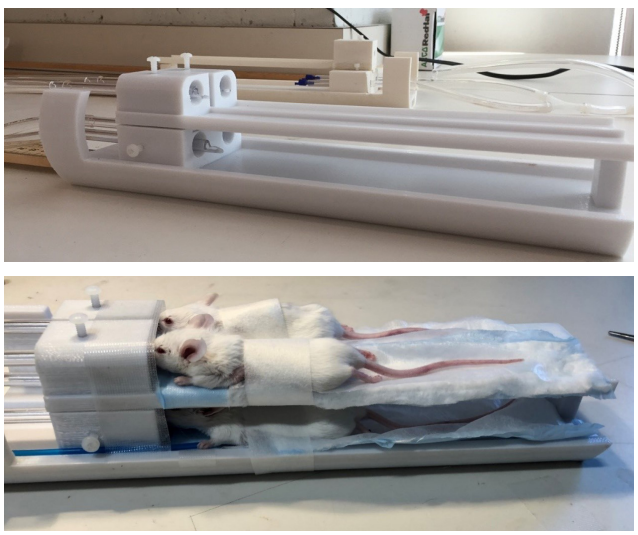

Figure 2 Custom designed 4 mouse bed (top) at Martinos Center for Biomedical Imaging, MGH. Top: bed without subjects on it to show the animal housing space and nose cone and tooth bar. Bottom: animal loaded with 4 mice prior an in vivo PET/MRI imaging session.

Mice were anesthetized with isoflurane (4% for induction,1 to 1.5% for maintenance in medical air). After placement of a tail vein catheter for probe administration, mice were positioned in a prone position on the multi-animal cradle. The cradle was manually positioned within the scanner for imaging. Animals were kept warm with an air heater system with the temperature and respiration rate monitored by a physiological monitoring system (SA Instruments Inc., Stony Brook NY) throughout the imaging session. The PET probe (100-200 μCi) was given intravenously as a bolus and followed by a 50 μL saline flush.

The scanner workstation is configured for acquiring simultaneous scans with parallel instances of ParaVision 6.1 (MR) and ParaVision 360 1.1 (PET). The interface is designed with a drag-and-drop function to import MR datasets to the paired PET dataset with the PV 360 1.1 interface for a common imaging processing interface for multi-modal datasets. Multi-modal image registration was completed using the PV 360 1.1 Geometric Registration function which operates on the basis a fusion calibration obtained for a multi-modal phantom. Data was then exported to DICOM format using the PV 360 1.1 DICOM export function. Image analysis was performing using PMOD v4.0 and AMIDE.

For initial whole-body PET/MR studies to evaluate the integrity of multi animal imaging, 10 MBq was injected in 3-mice and simultaneous PET and MR was completed. T1W 3D-Flash, T2W 3D-RARE, and T2 2D-RARE protocols were initially assessed.

After this verification, the 4-mouse study was carried out. For whole body MR + dynamic PET studies a Turbo RARE (TE 45 ms, TR 800 ms FA 90, Matrix 260 x 340 x 50 and a voxel spacing of 0.25 x 0.25 and 1 mm) protocol was used. DCE and a Dixon based sequences for fat/water imaging have also been employed. The PET data first was reconstructed as single dataset using MLEM, 12 iterations and 0.75 mm isotropic voxels. The following time bin schedule was used then used: 10 x 60 s; 10 x 180 s; 5 x 600 s.

Results

Initial pilot studies were performed to assess multi-mouse whole body imaging. An example 3 mouse dataset is shown in Figure 3. A 15-minute static PET and MR scans (TW1 3D-FLASH, T2W 3D-RARE, and T2W 2D-RARE) were performed. Multiple MR protocols were routinely run over the course of PET scans for maximum efficiency. PET and MR were found to be uncompromised for multi-animal imaging relative to single animal imaging. Mouse organs and detailed anatomical features in PET and MR registrations were well aligned. Further, the anesthesia and animal care setup supplied were found to be suitable for multi-mouse imaging and provide stable vitals and motion.

Figure 3

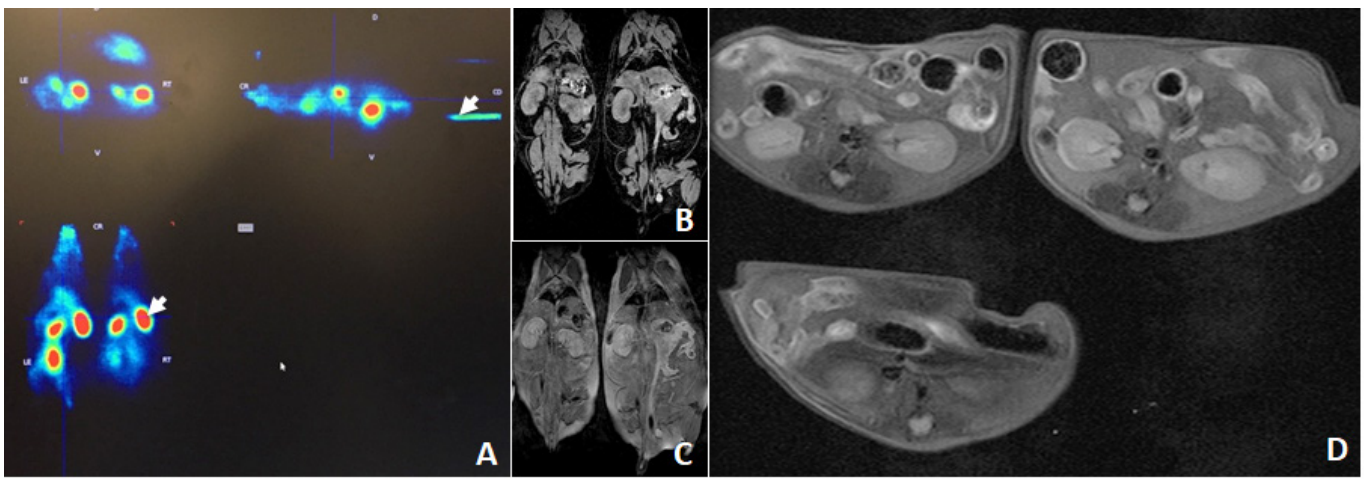

Figure 3 A) 68Ga PET B) T1W 3D FLASH, C) T2W 3D RARE, D) T2W RARE

Figure 4

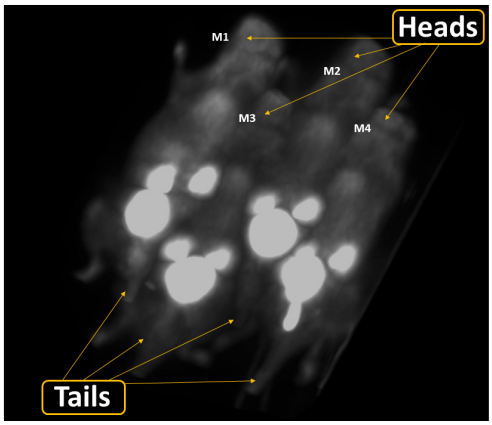

Figure 4. MIP of the whole PET dataset showing the 4 mice

Figure 4 shows a MIP view of a four-mouse dataset with 4 animals in the FOV. The profile of their entire bodies can be seen with the kidneys and the bladders visible as very hot

Figure 5 shows 6 time frames along the whole acquisition to show the biodistribution over time. The blue orthogonal cross-hairs that the image includes indicate in each case which slice is shown. The resolution within the coronal slice is higher than in the sagittal and transverse planes as the MRI acquisition has been planned this way. The PET fusion has the effect of re-sampling the original PET image for its resolution to match the MRI, used as the reference, and although the PET resolution is natively isotropic, here features the same lower resolution in the sagittal and transverse planes.

Figure 5

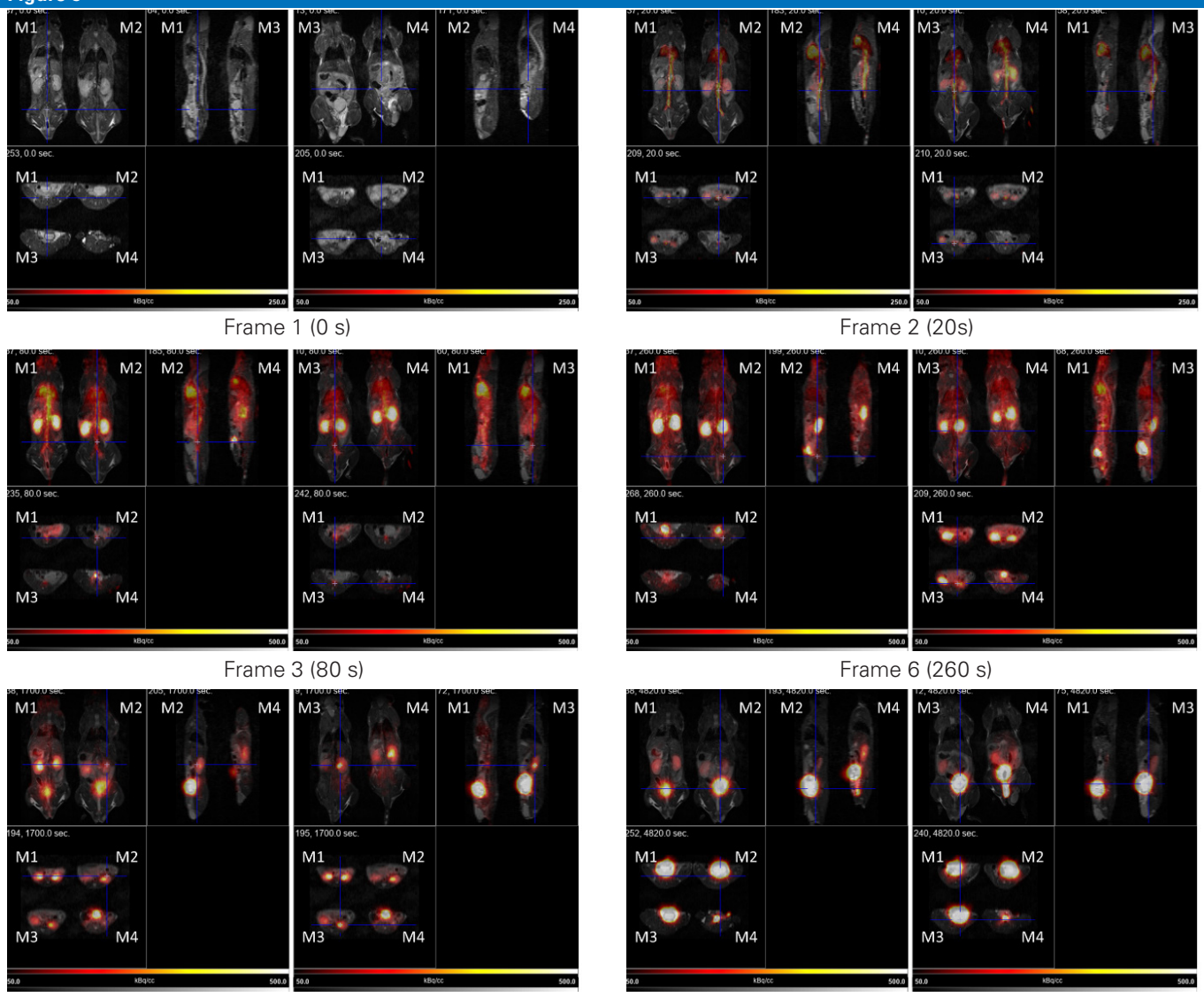

Figure 5. Frame 1, before the PET tracer is injected. Frame 2 showing most of the signal the inferior vena cava but with uptake in heart, lungs and kidneys

Frame 2 shows comprising 60 seconds worth of acquisition, from 20 seconds after the acquisition start to 80 seconds. The injection has occurred, and the tracer is already shown in to be present in the kidneys and the lungs as well as in the in the inferior vena cava through which the biodistribution started. Looking at the sagittal views significant uptake can be seen in the heart. Frame 3 comprises 60 seconds worth of acquisition, from 80 seconds from the acquisition start to 140 seconds. The tracer shows to be clearing fast through the kidneys but there is still high uptake in the heart, lungs and some uptake in the liver. Frame 6 shows the tracer to have distributed throughout the body. Frame 18 shows how the fast secretion rate is clearing the radiotracer from the body and the signal mainly concentrates in the kidneys and accumulates in the bladder. There is still some residual activity in rest of the body, note the lower threshold at 50 kBq/cc. The last frame shows that most of the signal comes from the kidneys and nearly all the activity is accumulated in the bladder

Figure 6

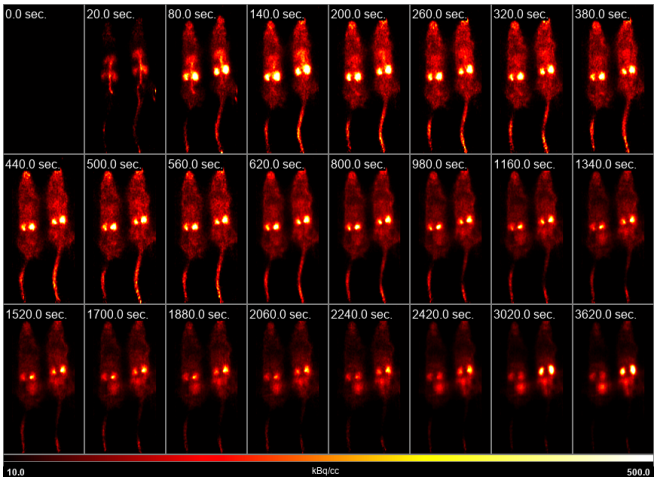

Figure 6. Axial slice through kidneys on the bottom 2 mice of the bed.

Figure 7

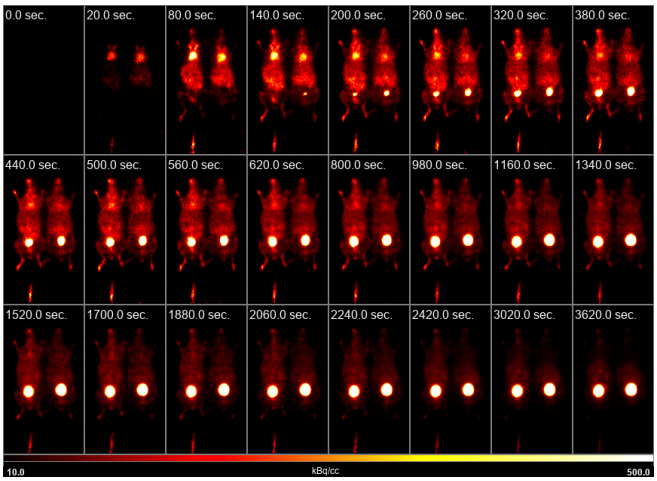

Figure 7 Axial slice through the heart on the top 2 mice of the bed.

Another useful way of visualizing the dynamic dataset I to plot a fix slice through time. Choosing a slice through the kidneys on the two mice of the lower floor, we can see how the uptake evolves through time (Figure 6).

To be able to show the progression through different organs, we choose an axial slice going across the hearts in the top two mice (Figure 7).

Exporting the image to DICOM and using PMOD, we can define 3D regions of interest following the contour of the organs as imaged by the MRI and extract the PET image values over time. In particular, we focused analysis on the heart and the liver (Figure 8).

Figure 8

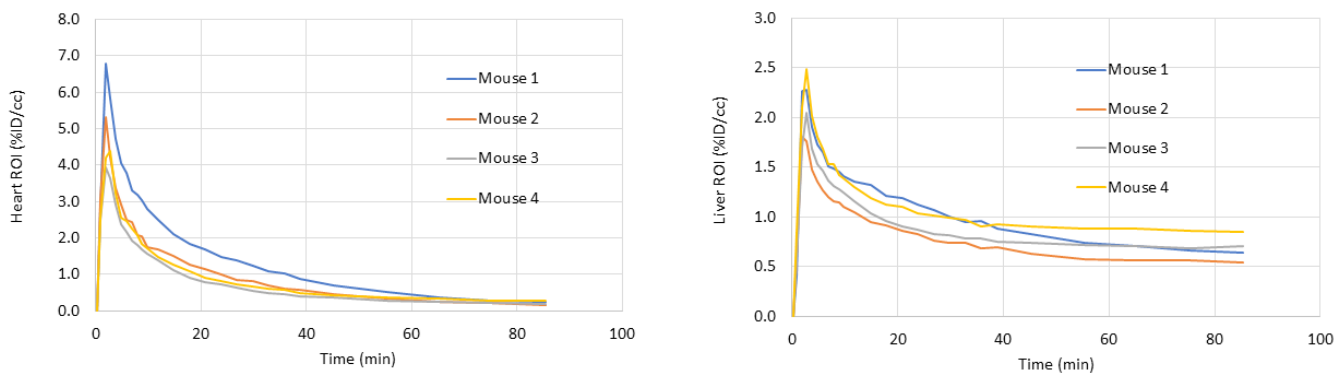

Figure 8 TAC for the heart and liver in each of the 4 mice.

Multi-Mouse PET/MR Neuroimaging

Method and material

Figure 9 shows the 6-mouse cradle developed at the Martinos Center for Biomedical Imaging for multi-modal PET/MR imaging using the system and workflow described above The 6-mouse cradle employed fused deposition modeling (FDM) on a Fortus printer using medical-grade polycarbonate-ISO material. These modular assemblies can be easily converted to accommodate 2, 4, or even 6 animals. The top mouse platform can be added or removed to the base assembly by using a positioning groove at the top of the base mouse nose bar holder or by dropping the top assembly into 4 tightly fitting corners provided by support bars on the lower assembly. Mouth bars were constructed by attaching 3D-printed mouth bars made of polycarbonate-ISO material to gas delivery tubes used halogen-free Garolite G-10 tubing (McMaster-Carr), which provides good strength with minimal wall thickness. In this bed the main gas delivery line splits into two feeding lines (one per side), with one line passing through the cradle base floor to reach the opposite side without causing additional obstruction in the scanner bore. The 6-mouse cradle multiplexed gas delivery to individual animals using YOOTOP 4-Way Aquarium Connectors to provide two 1:4 splitters. The cradle was manually positioning within the scanner for imaging. Animal respiratory monitoring was made using the SAI Model 1025T Monitoring and Gating system (Stony Brook, NY) and warm air was delivered to the scanner using the SAI MR-compatible Small Rodent Air Heater System. Gas flow rate was set to 1 ml/min using 1-1.5% isoflurane during scanning.

Figure 9

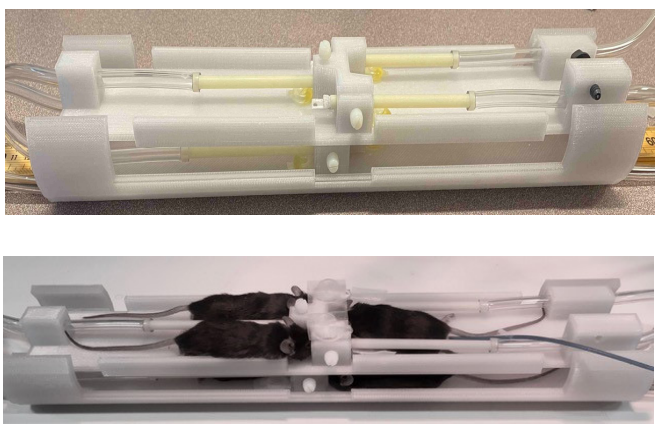

Figure 9. Custom designed 6 mouse bed (top) at Martinos Center for Biomedical Imaging, MGH. Top: bed without subjects on it to show the animal housing space and nose cone and tooth bar. Bottom: animal loaded with 6 mice prior to an in vivo PET/MRI imaging session.

Mouse PET presents challenges in terms of resolution and sensitivity. For instance, the entire volume of lateralized striatum is only about 12 mm^3, see ref. 2, or about 2 mm in a one dimension. Achieving true tracer doses of radioligand with adequate sensitivity is extremely challenging, and typically a tradeoff is made between sensitivity and mass dose, ref. 3.

Using our 6-animal cradle, we performed dynamic 11C-raclopride studies using within-scan challenges to test our ability to achieve adequate spatial detail and sensitivity. Tail vein catheters were used for injection of radiotracer at an average dose of 248 ± 43 mCi. In three of the six mice, a second tail vein was inserted for injection of 0.6 mg/kg amphetamine at 40 minutes into the scan. Time series for individual mice were extracted from the 4-dimensional dataset and aligned to the Allen Mouse Brain atlas space, and then analyzed using a linear-model SRTM-variant that includes a challenge term.

Results

Figure 10 shows multi-animal scan data (left) together with a group parametric map of baseline (pre-challenge) binding potential analyzed by an SRTM-based method after spatial normalization. Striatum is well separated from the Harderian glands.

Figure 10

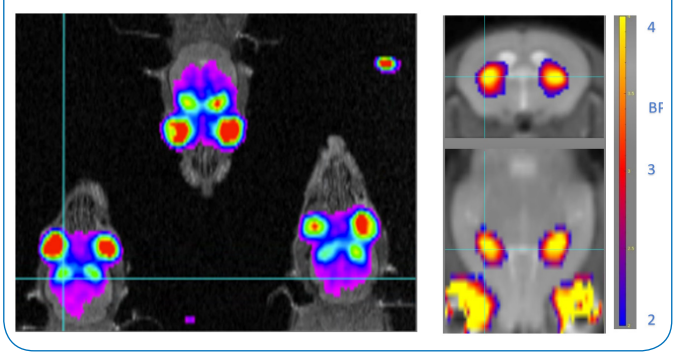

Figure 10 LEFT: Time-averaged [11C]-raclopride PET signal intensity overlaid on MRI for three animals on one level of the 6-animal cradle. RIGHT: A parametric map of D2/D3 receptor binding potential (BPND) for one animal, showing good spatial discrimination of specific binding in striatum.

Figure 11 shows a time-series analysis to determine the change in binding potential at 40 minutes with and without amphetamine challenge. Results demonstrate that sufficient low doses of radiotracer mass can be injected to achieve rough tracer conditions while maintaining adequate sensitivity. This capability facilitates efficient studies including the ability to perform within-scan challenges.

Figure 11

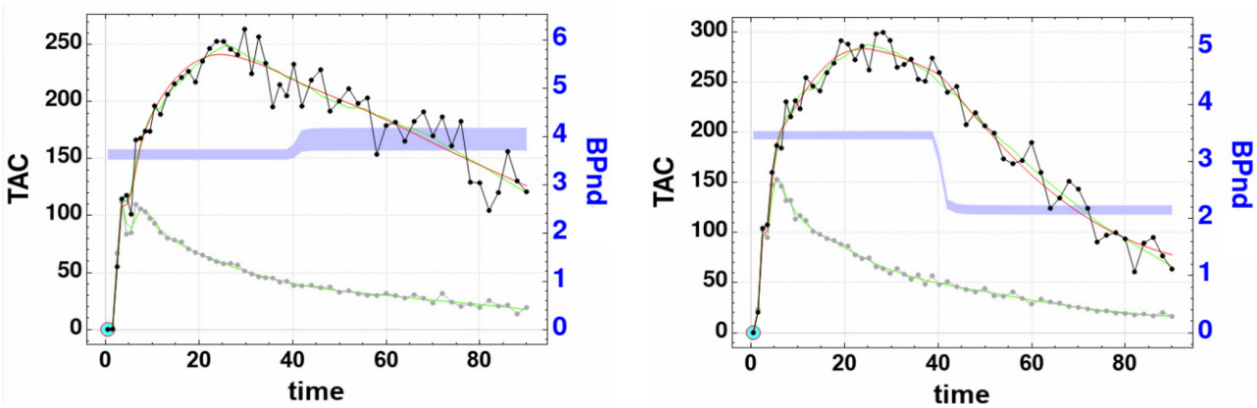

Figure 11 Time-series analysis of within-scan change using no real challenge (LEFT) or 0.6 mg/kg amphetamine (RIGHT) at 40 minutes into the scan. The estimate of binding potential is shown by the blue error envelope. Results are averaged across multiple animals within a single scan and illustrate the ability to perform within-scan challenges in mice using group scanning cohorts.

Figure 12

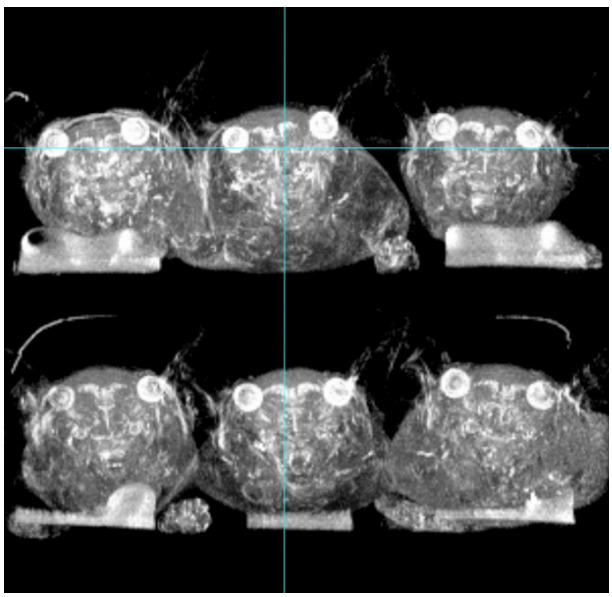

Figure 12. MIP views of the MRI image. The image is split in two rows to be able to show all 6 mice.

Multi-rat PET/MR Neuroimaging

Method and material

KORs are the most abundant opioid receptor in the human brain and hold potential as a target for nonaddictive analgesics. The more well-known opioid receptor, mu (MOR), is the target of potent analgesics such as oxycodone, morphine and fentanyl, producing powerful analgesia but also eliciting dangerous side effects such as addiction and respiratory depression. Activation of KOR also produces analgesia, but unlike MOR, it does not activate the brains reward system, the primary mechanism leading to addiction. As novel KOR-targeting drugs are being developed, confirming target-engagement in the living brain is a crucial step in drug development. In psychoactive drug discovery, titrating drug occupancy to maximize efficacy while avoiding undesirable side effects, is paramount to successful translation into humans. Our group has been studying KOR brain PET methods for measuring drug occupancy of KOR-targeting drugs in the living brain.

To study KOR agonist drug occupancy in vivo with PET we use the KOR-specific C-11 PET radiotracer [11C]GR103545. Unfortunately the short half-life of C-11 adds logistical challenges to conduct small animal PET scans, particularly to accomplish sufficient sample size for statistical significance. To circumvent this problem, we set out to accomplish imaging multiple rats from a single PET radiosynthesis with short-lived isotopes (e.g., carbon-11). We designed a scan bed that could accommodate 2 rats for brain imaging. With the transaxial limitations, side-by-side configuration would not be possible. Therefore, we designed and constructed scan platforms that would allow two rats with overlap at the head (side-by-side) when the animals were placed in an antiparallel orientation – head-first prone and tail-first prone. With this configuration, both heads would be at the isocenter of the PET and MR coil and custom bite bars and anesthesia nose cones would supply gaseous anesthesia to each animal from a central line and "Y" splitter. One potential issue that could result from anti-parallel orientation is a long intravenous extension line with significant void volume (particularly for the tail first prone animal). Fortunately, 61" extension lines are available commercially (Smiths Medical) with only 0.3 mL void volume, allowing sufficient length for injections while animals are placed in the scanner.

Kappa opioid receptor brain imaging of 2 rats (side by side anti-parallel) was conducted with 80min dynamic PET acqui-

sition following pretreatment with drug and a bolus of [11C] GR103545. MR scans were acquired for neuroanatomical colocalization (T2w RARE).

Figure 14 shows a 2-rat cradle developed at the Martinos Center for Biomedical Engineering for multi-modal PET/MR imaging using the system. The bed components were 3D printed using standard technologies. In this design, a long support structure is needed to hold the full body of both rats whose heads lie side by side in a manner such that are located on the same cross section. This not only saves space but guaranties that the brains can be located in the center of the PET FOV where sensitivity peaks.

The rats were anesthetized with isoflurane (4% for induction,1 to 2% for maintenance in medical air). The cradle was manually positioning within the scanner for imaging. After placement of a tail vein catheter for probe administration, mice were positioned in a prone position on the multi-animal cradle. Animals were kept warm with an air heater system with the temperature and respiration rate monitored.

Figure 14

Figure 14. 2-rat bed for neuro imaging. Top shows the 3D view of the CAD design. Middle image shows the whole length of the bed with full rat bodies and the bottom image shows a close up of the nose cones and heads. This set-up is capable of accommodating 2 rats with animal weights up to 0.5 kg each.

Results

Figure 15 shows the resulting images of the experiment. The top row shows the MRI of the two heads side by side, the middle row the PET image and the bottom shows the PET/MRI fusion.

To estimate drug occupancy in the brain, PET data was analyzed with kinetic modeling to calculate binding potential with respect to nondisplaceable uptake (BP_{ND}) using the Logan Reference model. The cerebellum was used as a reference region. Drug occupancy was calculated by the following:

$$\%O = \frac{(baseline\ BPnd) - (postdrug\ BPnd)}{baseline\ BPnd}$$

Figure 15

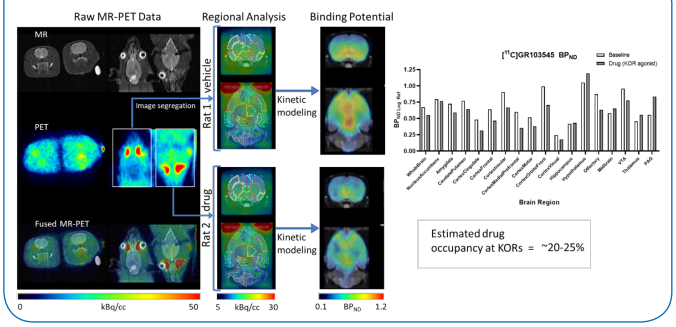

Figure 15. PET/MRI of the 2 rat experiment. Rats were pretreated with either vehicle (rat1) or drug (rat2) prior to administration of [11C]GR103545 bolus and 80 minute dynamic PET. Image data was segregated and coregistered to a brain template for regional analysis and kinetic modeling to calculate binding potential (BP_{ND}). At the dose utilized in this experiment, we estimated ~20-25% drug occupancy at KORs in the brain.

Conclusions

Preclinical PET plays a critical role in tracer development, with tracers typically initially evaluated in small test batches before scaling up production. Researchers in preclinical PET frequently attempt to maximize efficiency by performing multi-animal PET scans. This is especially important for short lived isotopes, but the need to maximize throughput also applies to longer lived isotopes. Some commercial vendors have begun offering solutions for multi-animal imaging, but many researchers have unique requirements for specific applications and the advent of 3D printing and prototyping has led some to begin developing custom solutions for multi animal-imaging.

PET/MRI offers unique characteristics making it a valuable tool in investigating disease models and target drugs in a broad range of applications. Here, we report on the application of PET/MRI in a range of high throughput studies ranging from 2 rats with side by side heads to mouse experiments with 3, 4 and up to 6 animals. The results demonstrated here indicate that sufficient resolution and sensitivity can be achieved with such multi-animal systems and can be employed in routine experiments.

References

1. Willy Gsell, Cesar Molinos, Carlos Correcher, Sarah Belderbos, Jens Wouters, Sven Junge, Michael Heidenreich, Greetje Vande Velde, Ahmadreza Rezaei, Johan Nuyts, Christopher Cawthorne, Frederik Cleeren, Lise Nannan, Christophe M. Deroose, Uwe Himmelreich, Antonio J. Gonzalez. *Characterization of a preclinical PET insert in a 7 Tesla MRI scanner: beyond NEMA testing.* Physics in Medicine & Biology July 2020.
2. Rosen GD, Williams RW. Complex trait analysis of the mouse striatum: independent QTLs modulate volume and neuron number. BMC Neurosci. 2001;2:5. doi: 10.1186/1471-2202-2-5. Epub 2001 Apr 17. PMID: 11319941; PMCID: PMC31432.
3. Kristina Fischer, Vesna Sossi, Andreas Schmid, Martin Thunemann, Florian C Maier, Martin S Judenhofer, Julia G Mannheim, Gerald Reischl, Bernd J Pichler. J Nucl Med. 2011 Jul;52(7):1133-41. doi: 10.2967/jnumed.110.086942. Epub 2011 Jun 16. Noninvasive Nuclear Imaging Enables the in Vivo Quantification of Striatal Dopamine Receptor Expression and Raclopride Affinity in Mice.
4. Willy Gsell, Cesar Molinos, Carlos Correcher, Michael Heidenreich, Joren Vandengaer, Wouter Oosterlinck, Uwe Himmelreich, Christophe DeRoose and Arno Nauerth. *PolyGate: benefits of a spatially resolved navigator (PolyGate) for self-gating cardiac imaging in multiple rodents.* Proc Intl. Soc. Mag. Reson. Med. (2019) 27: 2196.
5. Ignacio Muñoz-Criado, Jose Meseguer-Ripolles, Maravillas Mellado-López, Ana Alastrue-Agudo, Richard J Griffeth, Jerónimo Forteza-Vila, Ramón Cugat , Montserrat García and Victoria Moreno-Manzano. *Human Suprapatellar Fat Pad-Derived Mesenchymal Stem Cells Induce Chondrogenesis and Cartilage Repair in a Model of Severe Osteoarthritis.* Stem Cells Internatinal 2017 Volume 2017 |Article ID 4758930
6. Molinos Cesar, Sasser Todd, Salmon Phil, Gsell Willy, Viertl David, Massey James C., Miñczuk Krzysztof, Li Jie, Kundu Bijoy K., Berr Stuart, Correcher Carlos, Bahadur Ali, Attarwala Ali A., Stark Simon, Junge Sven, Himmelreich Uwe, Prior John O., Laperre Kjell, Van Wyk Sonica, Heidenreich Michael. *Low-Dose Imaging in a New Preclinical Total-Body PET/CT Scanner, Frontiers in Medicine,* Vol 6, 2019

Bruker BioSpin
info@bruker.com
bruker.com

Addendum: Bruker Multi-Animal Cradle

Professional solutions for multi-animal imaging also exist. Figure 2 shows Bruker's current multi-animal bed designed to fit up to 3 mice. See figure A1. This bed is compatible with all new PET/MRI instruments in addition to Bruker's latest PET/CT system, the PET/CT Si78 and Bruker's trimodal system, the Albira Si PET/SPECT/CT. This bed offers a number of advantages with respect other costumed made designs. The most important is probably a careful consideration to animal handling. A different anesthetic gas line can be fed to each of the animals. This potentially allows the control of anesthetic percentage to each animal when used with as many isoflurane vaporizers. In addition, each of the three animals' temperature and respiration can be monitored although again this will require as many monitoring kits as animals are imaged. By being an enclosure, animal warming can be supplied efficiently, and the air sucked out and filtered before venting in the laboratory atmosphere.

Figure A1

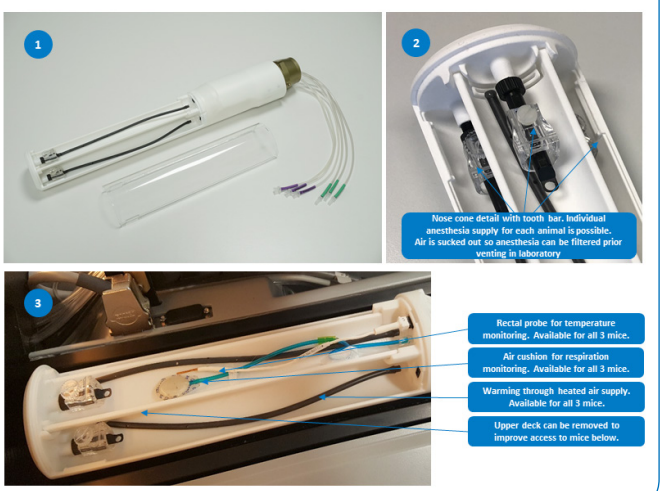

FigureA1. Advanced 3-mouse bed sold by Bruker. Image 1 shows the whole bed. Image 2 shows a details of the noise cone with the tooth bar. Image 3 shows a sample of the animal monitoring possibilities.

The Bruker multi-mouse bed comes is designed to fit the Animal Transport System. See in Figure A2 the bed with 3 mice as it enters a PET/MR 3T system automatically managed by the Animal Transport System. This standard connection makes it easy to fit it and achieves a good management of cables and ports. See Figure A2 how all lines are well tied up inside the energy chain.

Figure A2

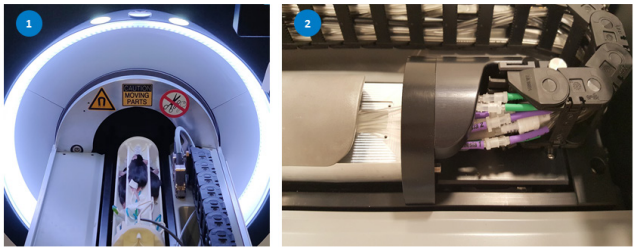

Figure A2. Image 1 shows the multi-animal bed entering the bore of a PET/MRI 3T. Image 2 shows the good management of the multiple cables and tubes required.

Selected Application Examples

F18 FDG PET/CT in mice

Bruker's 3 mouse bed presented here is also compatible with the PET/CT Si78 by Bruker. A PET/CT experiment in mice injected with F18 FDG was carried out. F18 FDG, a glucose analogue, is the most common radiopharmaceutical in PET imaging. The Si78 features a CT subsystem capable of imaging total body mice in less than 10 seconds as well as imparting a very low dose. The PET subsystem has essentially the same capabilities of the PET integrated with MRI systems. Figure A4 shows a 3D rendering view of the resulting PET/CT dataset. The dissimilar tracer distribution is explained by the different activities and injection times used in each animal. The CT acquisition took around 10 seconds and the PET 30 min.

Figure A4

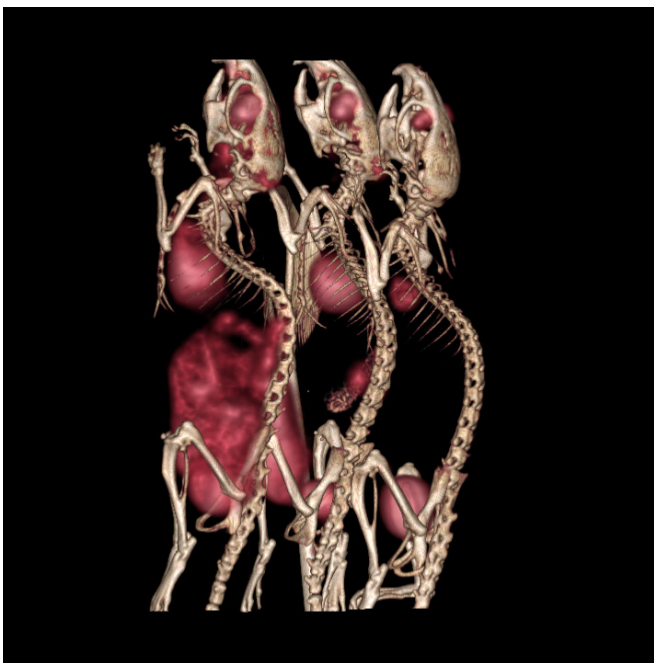

Figure A4. F18FDG PET/CT of 3 mice with the PET/CT Si78.

Low dose imaging: F18 NaF PET

F18 NaF is a common tracer in the clinic to investigate cancer spread in the bones. In preclinical imaging, F18 NaF has been used to monitor bone joint disorders including osteoarthritis, see ref. 5. A F18 NaF scan is also sometimes used to demonstrate in-vivo resolution of preclinical PET systems. Figure A5 was extracted from ref. 6 where C Molinos et al carried out an evaluation the low dose performance of the new Bruker PET/CT system Si78. Bruker multi-animal bed was employed in such a study.

Figure A5

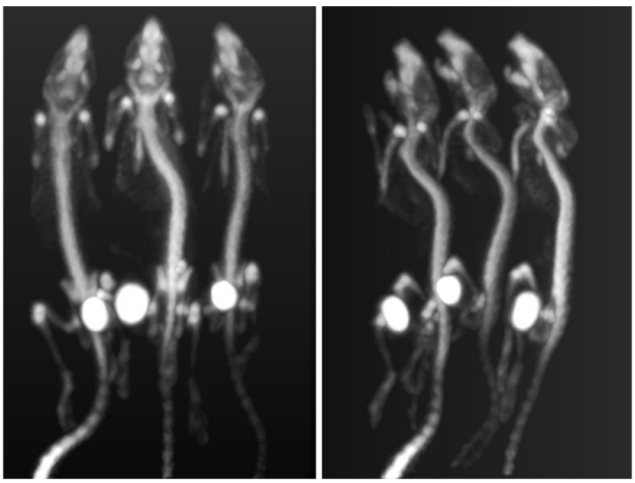

Figure A5. Low dose F18 NaF imaging of three mice. Each animal was injected with 2 MBq and the acquisition lasted 18 minutes.

PET/MRI Cardiac Imaging

Gsell et al. demonstrated the possibility to use MRI information for retrospectively reconstruct cardiac gated PET data first with a single animal and then as an extension of the method with as many as 3 (ref. 4, the method is not commercially available yet). This is possible thanks to the synchronization of PET/MRI electronics and has the obvious advantage of not requiring ECG electrodes hence simplifying the animal handling and avoiding corruption of gating by noise from gradient switching. The method with the implementation of spatially resolved navigator (PET/MRI PolyGate), enables the extraction of the cardiac and respiratory motions of each separate animals at retrospectively reconstruct cardiac gated PET data. The figure below shows the result of reconstructed the same 18 FDG PET/MRI dataset three times applying the retrospective PET sorting to each one of the 3 animals.

Figure A3

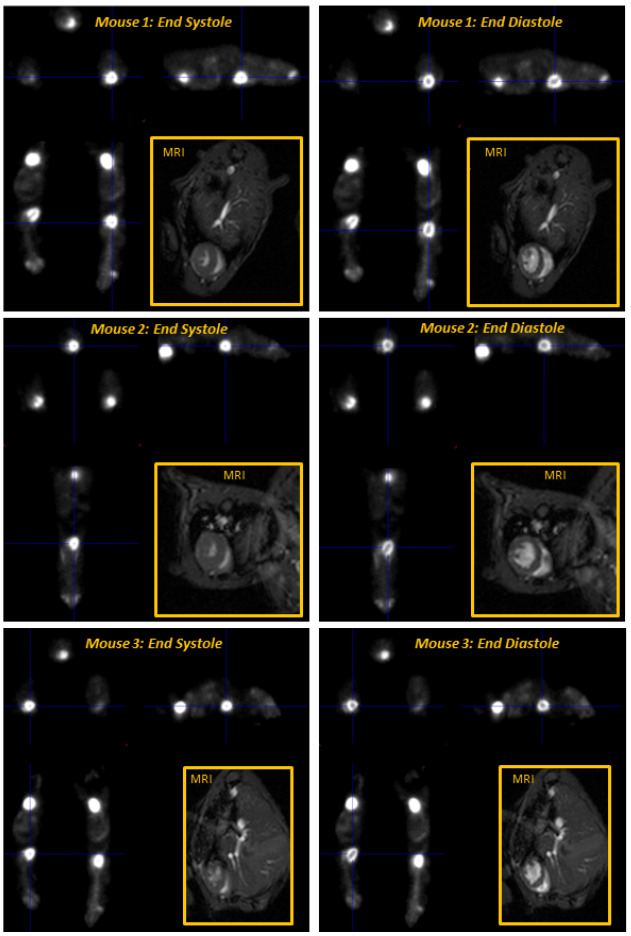

Figure A3. PET/MRI in 3 mice without the need of ECG electrodes. See ref. 4 Gsell et al.